論文 / 著書情報
Article / Book Information

論題	
Title	Vibrations Suppression Control of Image Transfer Belt System with Flywheel or Dynamic Vibration Absorber
著者	Yu Jie, 山浦 弘, 大石 剛弘
Author	Jie Yu, Hiroshi Yamaura, Takehiro Oishi, Yimei Yu
掲載誌/書名	, Vol. 7, No. 1, pp. 52-64
Journal/Book name	Journal of Advanced Mechanical Design, Systems, and Manufacturing, Vol. 7, No. 1, pp. 52-64
発行日 / Issue date	2013, 2
URL	http://search.ieice.org/
権利情報 / Copyright	本著作物の著作権は日本機械学会に帰属します。
Note	このファイルは著者（最終）版です。 This file is author (final) version.

JSME
Technical Journal

Vol.X, No.X, XXXX

Vibration Suppression Control of Image Transfer Belt System with Flywheel or Dynamic Vibration Absorber*

Jie YU**, Hiroshi YAMAURA***, Takehiro OISHI† and Yimei YU††

** Tokyo Institute of Technology, Department of Mechanical and Control Engineering
2–12–1 O-okayama, Meguro-ku, Tokyo, 158-8552, Japan
E-mail: yu.j.ad@m.titech.ac.jp

*** Tokyo Institute of Technology, Department of Mechanical and Control Engineering
2–12–1 O-okayama, Meguro-ku, Tokyo, 158-8552, Japan
E-mail: yamaura@mech.titech.ac.jp

† Fuji Xerox Co., Ltd.
430 Sakai, Nakai-machi, Ashigarakami-gun, Kanagawa, 259-0157, Japan
E-mail: takehiro.oishi@fujixerox.co.jp

†† Fuji Xerox Co., Ltd.
430 Sakai, Nakai-machi, Ashigarakami-gun, Kanagawa, 259-0157, Japan
E-mail: yu.yimei@fujixerox.co.jp

Abstract

The purpose of this study was to investigate vibrations suppression control methods of image transfer belt system which is widely applied in image formation procedure of printers and copy machines. The study focused on vibrations caused by loading torque of printing medium when delivered into the machinery. The system was modelled as a four-rollers-belt with a stepper motor based on exist apparatus. Equations of motion and vibration of the four-rollers-belt system were established. Two types of description about the vibration in image forming part of belt, stretching displacement and absolute displacement were selected as main inhibited quantities. Impacts on the two quantities by several parameters of the system, including *Young's* modulus of belt, rotational stiffness of motor coupling were studied. Additional flywheels and dynamic absorbers were used to improve the system performance, and an evaluation function was defined to estimate the effects. The results indicated that the two devices reduced the two displacements, and the outcomes varied as different attached locations and moment of inertia. It confirmed that by adding a flywheel with large inertia on burden roller, or a dynamic vibration absorber on drive roller could achieve better suppression results.

Key words : intermediate transfer belt (ITB), vibration suppress, flywheel, dynamic vibration absorber, printer, mode separation

1. Introduction

Printing is a competitive and worldwide industry since printers and copy machines have been widely used in modern office document processing. For high-speed printing technology, electrophotography (EP) or xerography is the technology of choice(?,). Due to the increment in market demand for color products, technological challenges in achieving high-quality print-outs have been significantly increased.

Xerography is a dry photocopying technique invented by *Chester Carlson* in 1938, and it is the foundation technology for laser printers and photocopiers to come. There are six basic steps during a conventional xerography process: charging, exposure, developing, transferring, fusing, and cleaning. Each step relates to print quality for a xerography printer. As the increasing demand for high-speed color printing, the intermediate transfer belt (ITB) has been generally applied in image forming and transfer process. Instead of transferring the image

*Received DD MM, YYYY (No. 01-2345)
[DOI: 10.1299/jamdsm.X.1]

onto printing medium directly, a belt passes through multiple different color imaging stations positioned in series along the circumference to create a full-color image on its surface(?,). The full-color image is then transferred from the ITB to printing medium. Therefore each color planes formed on the ITB is closely related to the final printing quality. A general problem associated with this process is the misregistration or misalignment of one or more of the color planes. Researches have shown that mechanical components can induce vibration or transmission deviation, which can cause the misalignment(?),(?,). And among these many factors, the loading torque of printing medium when transferred into printers has been one of the disturbances.

Many methods have been investigated to prevent the misalignment, and they have achieved some efforts. Some researches have focused on improving structure, for example, providing an ITB having one or more steering ribs formed into the belt to prevent it from slipping on the drive roller or prevent a zig-zag motion(?,). Others have been conducting velocity control of stepper motor and photoconductive drum with plant disturbance included generally(?),(?,). However, little has been documented in the attenuation or cancellation of vibrations caused by loading torque of printing medium specifically through additional apparatuses. An advantage of velocity control is its ability to reduce system sensitivity to uncertainties. But with a single actuator, expectation can not be achieved. Moreover the complication of the printers without detailed model aggravates the design.

In this paper, a four-rollers-belt system model with excitation force was proposed to simplify the existing ITB system. Mathematical descriptions were established based on the model, and influences of several parameters on the system were studied. Instead of complex controller, the flywheel and dynamic vibration absorber were introduced to the system to inhibit the vibration especially in the image forming part of the ITB. Several cases were studied through changing the attaching location and moment of inertia of the devices. Results indicated that rotational stiffness between drive roller and stepper motor could reduce the vibration. And an evaluation function defined in this study pointed out that by adding a flywheel with large moment of inertia on burden roller, or a dynamic vibration absorber on drive roller both could succeed in the desired consequences.

2. Nomenclature

E : *Young's* Modulus of belt
A : Crossing area of belt
x_t : Displacement of the tension apparatus
k_t : Stiffness of the tension apparatus
α, β : Angular position of the tension apparatus
m_2 : Mass of tension roller
θ_m : Rotational angular of stepper motor
$\ddot{\theta}_m$: Angular acceleration of stepper motor
$\theta_i (i = 1, 2, 3, 4)$: Rotational angular of roller
$\ddot{\theta}_i (i = 1, 2, 3, 4)$: Angular acceleration of roller
$r_i (i = 1, 2, 3, 4)$: Radius of roller
$I_i (i = 1, 2, 3, 4)$: Inertia of roller
$k_i (i = 1, 2, 3, 4)$: Stiffness of belt
$l_i (i = 1, 2, 3, 4)$: Length of belt
k_m : Rotational stiffness between drive roller and stepper motor
T_L : Loading torque of printing medium
$[M], [K], [C]$: Mass, stiffness, damping matrices of the system
$[M_d], [K_d], [C_d]$: Modal mass, stiffness, damping matrices of the system
$[M_e], [K_e], [C_e]$: Effective mass, stiffness, damping matrices of the system
μ, λ : coefficient in Rayleigh damping model
μ_f, μ_a : inertia ratio of flywheel, dynamic vibration absorber
I_f : inertia of flywheel
I_a, k_a, c_a : inertia, stiffness, damping of dynamic vibration absorber
k_e, c_e : coefficient of dynamic vibration absorber

3. Modelling of Basic Four-Rollers-Belt System

A four-rollers-belt system was built up in this study as a simplified model of ITB system

in image forming apparatus, since effects of assistant rollers on the whole system were not so much significant. Equations of motion and vibration under three assumptions were obtained in this section. Follows was study about effects of parameters on the system. The excitation force modeling was also included in this part.

3.1. System Description

Figure 1 graphs the architecture of four-rollers-belt system that contained four main rollers, four parts of transfer belt, an additional tension apparatus, and a stepper motor. The four rollers that functioned most during image transfer process were named as: burden roller (BR) where the printing medium was carried into printers; tension roller (TR) where the tension apparatus was attached; drive roller (DR) which connected to a stepper motor that provided drive torque; adjust roller (AR) set as an assistant roller.

The following three assumptions were applied to simplify the mathematical expression

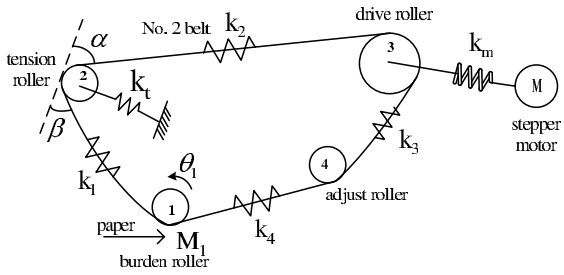

Fig. 1 Four-rollers-belt system

establishment:

(1) Each part of the belt was modeled as a spring.

(2) Slip between roller and belt was out of consideration.

(3) Stepper motor rotated in a constant angular speed.

Under assumption (1), the stiffness of belt was calculated as $k_i = \frac{EA}{l_i}$. Based on *Newton's Second Law* and assumptions above, the equations of motion were as follows:

$$\begin{aligned}
I_1\ddot{\theta}_1 &= -(\theta_1 r_1 - \theta_4 r_4)k_4 r_1 + (\theta_2 r_2 - \theta_1 r_1 + x_t \sin\beta)k_1 r_1 + T_L \\
I_2\ddot{\theta}_2 &= -(\theta_2 r_2 - \theta_1 r_1 + x_t sin\beta)k_1 r_2 + (\theta_3 r_3 - \theta_2 r_2 + x_t \sin\alpha)k_2 r_2 \\
I_3\ddot{\theta}_3 &= -(\theta_3 r_3 - \theta_2 r_2 + x_t sin\alpha)k_2 r_3 + (\theta_4 r_4 - \theta_3 r_3)k_3 r_3 + k_m(\frac{\theta_m}{m} - \theta_3) \\
I_4\ddot{\theta}_4 &= -(\theta_4 r_4 - \theta_1 r_1)k_4 r_4 + (\theta_3 r_3 - \theta_4 r_4)k_3 r_4 \\
m_2\ddot{x}_t &= -k_t x_t - (\theta_2 r_2 - \theta_1 r_1 + x_t \sin\beta)k_1 \sin\beta - (\theta_3 r_3 - \theta_2 r_2 + x_t \sin\alpha)k_2 \sin\alpha
\end{aligned} \tag{1}$$

Rotational angular speed can be separated into static part and vibration part: $\dot{\theta}_i = \bar{\dot{\theta}}_i + \Delta\dot{\theta}_i$ $(i = 1, 2, 3, 4, m)$, therefore rotational angular and acceleration were changed into: $\theta_i = \dot{\theta}_i t + \Delta\theta_i$, $\ddot{\theta}_i = \Delta\ddot{\theta}_i$ $(i = 1, 2, 3, 4, m)$.

Also under steady rotation status and assumption (2) the following equation was valid: $r_i\bar{\dot{\theta}}_i = r_j\bar{\dot{\theta}}_j$ $(i, j = 1, 2, 3, 4,\ i \neq j)$.

Equations of vibration of the system were obtained by substitute the formulas above into equation (1):

$$\begin{aligned}
I_1\Delta\ddot{\theta}_1 &= -(\Delta\theta_1 r_1 - \Delta\theta_4 r_4)k_4 r_1 + (\Delta\theta_2 r_2 - \Delta\theta_1 r_1 + x_t \sin\beta)k_1 r_1 + T_L \\
I_2\Delta\ddot{\theta}_2 &= -(\Delta\theta_2 r_2 - \Delta\theta_1 r_1 + x_t sin\beta)k_1 r_2 + (\Delta\theta_3 r_3 - \Delta\theta_2 r_2 + x_t \sin\alpha)k_2 r_2 \\
I_3\Delta\ddot{\theta}_3 &= -(\Delta\theta_3 r_3 - \Delta\theta_2 r_2 + x_t sin\alpha)k_2 r_3 + (\Delta\theta_4 r_4 - \Delta\theta_3 r_3)k_3 r_3 - k_m\Delta\theta_3 \\
I_4\Delta\ddot{\theta}_4 &= -(\Delta\theta_4 r_4 - \Delta\theta_1 r_1)k_4 r_4 + (\Delta\theta_3 r_3 - \Delta\theta_4 r_4)k_3 r_4 \\
m_2\ddot{x}_t &= -k_t x_t - (\Delta\theta_2 r_2 - \Delta\theta_1 r_1 + x_t \sin\beta)k_1 \sin\beta - (\Delta\theta_3 r_3 - \Delta\theta_2 r_2 + x_t \sin\alpha)k_2 \sin\alpha
\end{aligned} \tag{2}$$

Equation (2) was transformed into matrix form by defining vector: $x = [\Delta\theta_1, \Delta\theta_2, \Delta\theta_3, \Delta\theta_4, x_t]^{\mathrm{T}}$, and it was expressed as: $[M]\ddot{x} + [K]x = [P]T_L$. This matrix formula was purely based on phys-

ical principle and excluded the damping factor that exists in dynamic analysis of structures and foundations. Most damping is caused by viscosity in reality, and Rayleigh damping model is widely applied to researches.

The framework of Rayleigh damping model is that the damping factor is a linear combination of mass factor and stiffness factor from a system. And it is shown as follows: $[C] = \mu[M] + \lambda[K]$. μ, λ were calculated from experimental data in this study. The values were $\mu = 25$, and $\lambda = 3 \times 10^{-4}$. Therefore the equation of vibration of the four-rollers-belt system in matrix form was exhibited as:

$$[M]\ddot{x} + [C]\dot{x} + [K]x = [P]T_L \tag{3}$$

. According to suppression purpose, state variable vector and output vector were selected as below:

$$\begin{aligned} X &= \begin{bmatrix} x & \dot{x} \end{bmatrix}^{\mathrm{T}} \\ &= \begin{bmatrix} \Delta\theta_1 & \Delta\theta_2 & \Delta\theta_3 & \Delta\theta_4 & x_t & \Delta\dot{\theta}_1 & \Delta\dot{\theta}_2 & \Delta\dot{\theta}_3 & \Delta\dot{\theta}_4 & \dot{x}_t \end{bmatrix}^{\mathrm{T}} \\ Y &= \begin{bmatrix} y_1 & y_2 & y_3 & y_4 & y_5 & y_6 & y_7 \end{bmatrix}^{\mathrm{T}} \\ &= [r_1\Delta\theta_1 \;\; r_2\Delta\theta_2 \;\; r_3\Delta\theta_3 \;\; r_4\Delta\theta_4 \;\; x_t \\ &\quad \Delta\theta_3 r_3 - \Delta\theta_2 r_2 + x_t \sin\alpha \;\; \frac{1}{2}(\Delta\theta_3 r_3 + \Delta\theta_2 r_2 + x_t \sin\alpha)]^{\mathrm{T}} \end{aligned} \tag{4}$$

The last two items in output vector marked as y_6, y_7 represented stretching displacement and absolute displacement occurring in No. 2 belt. The stretching displacement described the stretching amount in the belt as a spring, and the absolute displacement represented the derivation amount from the centre point. They were the main quantities to be reduced in this study.

The state space equations of the four-rollers-belt system were expressed as:

$$\begin{aligned} \dot{X} &= \mathbf{A_{mtr}}X + \mathbf{B_{mtr}}T_L \\ Y &= \mathbf{C_{mtr}}X + \mathbf{D_{mtr}}T_L \end{aligned} \tag{5}$$

3.2. Parameters Study

Generally, the length and area of each part of belt should remain constant but the material can change. Also the tension apparatus could be manual adjusted. Therefore effects of *Young's* modulus E, tension roller's mass m_2, stiffness of the spring k_t, and the rotational stiffness between drive roller and motor k_m on the system were investigation objects in this section. Table (1) exhibited value of each parameter of the systme, and symbols in blue represented the standard value for the four subjects.

Figure 2.a, 2.b, 2.c, 2.d graphed the results under different parameter value separately,

Parameter	Symbol	Value
length of belt	l_i $(i = 1, 2, 3, 4)$	0.2 m
area of belt	A	3.6×10^{-5} (m^2)
radius of rollers	r_i $(i = 1, 2, 4)$	0.014 m
radius of drive roller	r_3	0.01675 (m)
inertia of rollers	I_i $(i = 1, 2, 4)$	6.45×10^{-5} (kgm^2)
inertia of drive roller	I_3	1.32×10^{-4} (kgm^2)
position angular	α, β	45 $(degree)$
Young's modulus	E	3.4×10^3 (MPa)
tension roller's mass	m_2	1 (kg)
stiffness of the spring	k_t	1.38×10^4 (N/m)
rotational stiffness	k_m	39 $(N \cdot m/rad)$

Table 1 Parameters of four-rollers-belt system.

and the maximum calculation angular frequency was $\omega_{max} = 5000 rad/sec$

Figures above indicated that stretching displacement was more vulnerable than absolute displacement. However larger rotational stiffness between DR and stepper motor could reduce

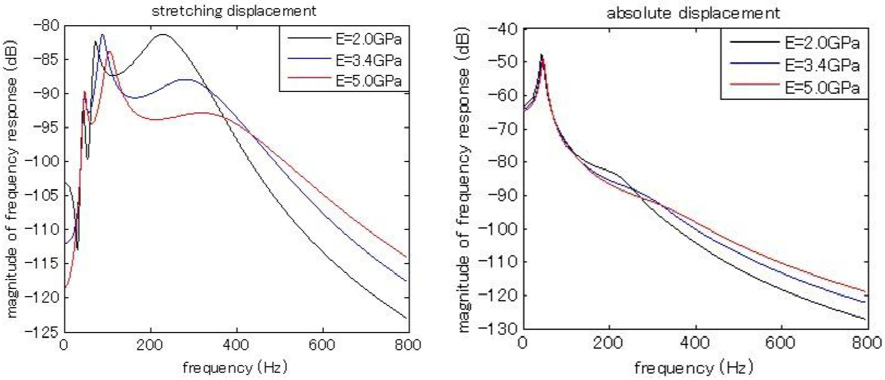

Fig. 2 System performance with different *Young's* modulus of belt

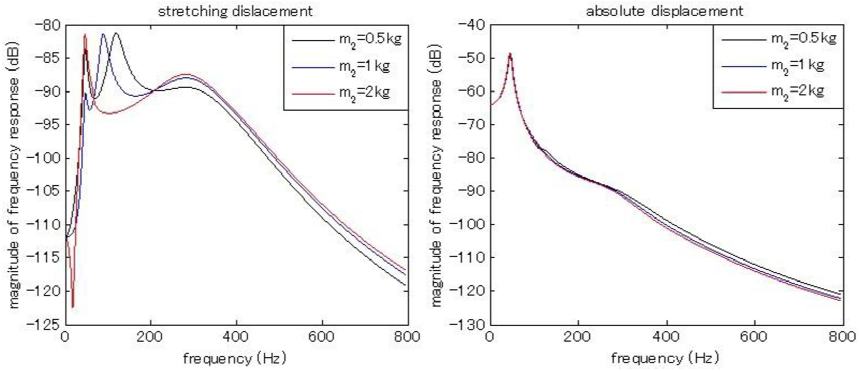

Fig. 3 System performance with different TR mass

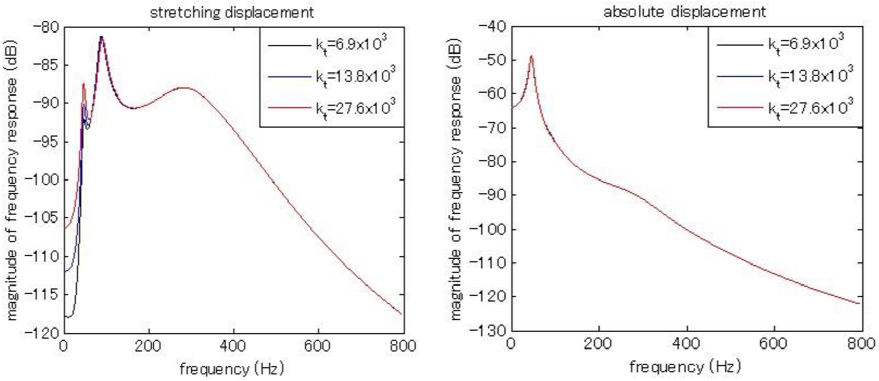

Fig. 4 System performance with different tension apparatus stiffness

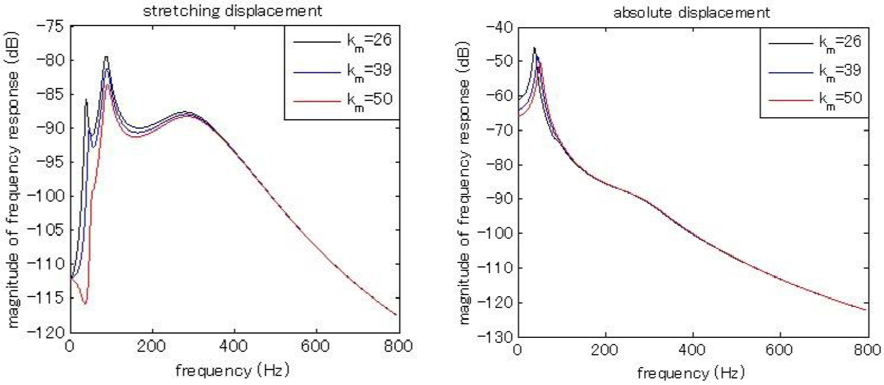

Fig. 5 System performance with different rotational stiffness between DR and stepper motor

both these two quantities. Also natural frequencies of the system varied as the parameters changed which satisfied physical principle.

3.3. Modelling of Excitation Force

The loading torque of printing medium was the excitation force to the four-rollers-belt system, and it was the disturbance to the system. Building up a model from mechanism is complicated due to the loading torque is related to many factors, such as printing speed, paper thickness, and material properties. Therefore a half sine function obtained from experimental data was used in this study, and the mathematical expression was:

$$T_L(t) = -0.5\sin(100\pi t) \;\; 0.1s \le t \le 0.11s \;\; \Delta t = 0.01s \tag{6}$$

The spacing time was 0.01 seconds, and the maximum loading torque was $0.5(N * m)$.

Fourier transformation was conducted on the excitation force in order to analysis with the frequency response of the four-rollers-belt system:

$$T_L(jw) = -\frac{50\pi}{\omega^2 - 100^2\pi^2}(\exp^{-0.11\,j\omega} + \exp^{-0.1\,j\omega}) \tag{7}$$

4. Vibration Suppression Methods

Some parameters affect the performance of the system significantly according to results of parameters study. So vibration could be suppressed by adjusting the value properly. However most of the values were already fixed because of the production demand. On the other hand, the absolute displacement did not vary frequently. Therefore it was more feasible to reduce the vibration by adding suppression devices.

Flywheel and dynamic vibration absorber were chosen in this work due to their simply structure, low spending cost and high efficiency. Several cases including different attaching location and inertia of the device were investigate to find out optimum.

Flywheel is a rotating mechanical device that is used to store rotational energy. Flywheels have a significant moment of inertia, and thus resist changes in rotational speed. This device is widely used in vehicle industry due to the simply mechanism and low cost. The moment of inertia of drive roller which was almost twice of other rollers was chosen to the reference for flywheel: $I_f = \mu_f I_3$

4.1. Dynamic Vibration Absorber

The dynamic vibration absorber is classic engineering device, consisting of a mass, a spring and perhaps a damper, which is attached to a vibrating main system so as to attenuate it undesirable forced vibratory response.

The first mathematical treat of the passive dynamic vibration absorber, which is attached to an undamped force excited primary system, was given by *Ormondroyd* and *Den Hartog*. A detailed investigation and a discussion of optimal tuning and damping parameters is to be found in the well known book by *Den Hartog*. Figure X shows a simply constitution of dynamic vibration absorber attached to an undamped single-degree-of-freedom system:

m_1, k_1 is the mass and stiffness of main system, and m_a, k_a, c_a belong to dynamic

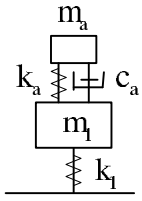

Fig. 6 Structure of dynamic vibration absorber on a SDOF system

vibration absorber. There are several parameters defined as follows:

$$\omega_1 = \sqrt{\frac{k_1}{m_1}},\; \omega_a = \sqrt{\frac{k_a}{m_a}},\; \mu_a = \frac{m_a}{m_1},\; \nu = \frac{\omega_1}{\omega_a},$$
$$\zeta = \frac{c_a}{2m_a\omega_a} = \frac{c_a}{2\mu_a\nu m_1\omega_1}$$

The optimal tuning condition is when:

$$\nu_{opt} = \frac{1}{1+\mu_a}, \quad \zeta_{opt} = \sqrt{\frac{3\mu_a}{8(1+\mu_a)}}$$

Combining formulas below, the optimal parameter for dynamic vibration absorber is:

$$\begin{aligned} m_a &= \mu_a m_1 \\ k_a &= \mu_a(1+\mu_a)^2 k_1 \\ c_a &= \frac{\mu_a}{1+\mu_a}\sqrt{\frac{3\mu_a k_1 m_1}{2(1+\mu_a)}} \end{aligned} \tag{8}$$

The parameters in the four-rollers-belt system was not substituted directly since the main system was a multi-degree-freedom one and the variables were combined with each others. By change full mass matrix, stiffness matrix and damping matrix into effective mass, stiffness, damping matrix, the system could be separated into several SDOF systems.

4.2. Mode Separation of Four-Rollers-Belt System

When the mass matrix is post-multiplied by the mode shape matrix $[\Phi]$, and pre-multiplied by its transpose $[\Phi]^{\mathrm{T}}$, the result is a diagonal matrix, shown below. It is definition of modal mass. This is also used to the stiffness matrix, and since the damping matrix is a linear combination of mass and stiffness matrix, the modal damping matrix is diagonal too.

$$[M_d] = [\Phi]^{\mathrm{T}}[M][\Phi], \quad [K_d] = [\Phi]^{\mathrm{T}}[K][\Phi], \quad [C_d] = [\Phi]^{\mathrm{T}}[C][\Phi]$$

The former coordination was converted to modal coordination $x = [\Phi]x_d$ and substituted into equation (4). The modal matrix form of the equation of vibrations was exhibited as:

$$[M_d]\ddot{x}_d + [C_d]\dot{x}_d + [K_d]x_d = [P_d]u \tag{9}$$

Each mode can be interpreted as a mass-spring-dashopot system in mode analysis. The following transform named effective matrices expression was conducted to guarantee the excitation force functioned united:

$$[M_e] = [P][P_d]^{-1}[M_d], \quad [K_e] = [P][P_d]^{-1}[K_d], \quad [C_e] = [P][P_d]^{-1}[C_d]$$

Finally the effective matrices expression of the four-rollers-belt system was indicated as:

$$[M_e]\ddot{x}_d + [C_e]\dot{x}_d + [K_e]x_d = [P]u \tag{10}$$

It meant the four-rollers-belt system that contained multiple degree of freedom was divided into five modes that was of single degree of freedom. Moreover since each SDOF system contained damping factor, the original calculation about parameters in dynamic vibration absorber should be adjusted. So the parameters of dynamic vibration absorber in this study should be calculated as:

$$\begin{aligned} I_a &= \mu_a I_3 \\ \mu_{ei} &= \frac{I_a}{I_{ei}} \\ k_a &= k_e \mu_{ei}(1+\mu_{ei})^2 k_{ei} \\ c_a &= c_e \frac{\mu_{ei}}{1+\mu_{ei}}\sqrt{\frac{3\mu_{ei}k_{ei}I_{ei}}{2(1+\mu_{ei})}} \end{aligned}$$

where k_e, c_e are the coefficient to adjust the value of stiffness and damping, μ_a is inertia ratio between dynamic vibration absorber and DR, μ_{ei} is the equivalent inertia ratio responding to each mode, and k_{ei}, I_{ei} are the effective stiffness and mass of the i-th mode respectively.

4.3. Evaluation Function

An evaluation function was defined in this part to appraise the suppression results of flywheel and dynamic vibration absorber. Based on the property of Fourier transform and linear time-invariant system, the magnitude of system output can be calculated by $|Y(j\omega)| = |H(j\omega)| \cdot |T_L(j\omega)|$, where $Y(j\omega)$ is the system output, $T_L(j\omega)$ is the loading torque, and $H(j\omega)$ is the frequency response of the system. $Y(j\omega)$ only reflected the information about the system and disturbance which irrelevant to human visual sensibility. Therefore a visual transfer function (VTF) from psychological evaluation was introduced in this study. And the evaluation function was defined as:

$$J_i = \frac{1}{2\pi}\int_0^{\omega_{max}} |Y(j\omega) * VTF(j\omega)|^2 d\omega \quad (i = 1, 2, 3, 4, 5, 6, 7) \tag{11}$$

J_6, J_7 that represented stretching and absolute displacement were mainly inhibited items.

5. Simulation Results

In this section, system behaviour with flywheel on different roller, or dynamic vibration absorber compensated to different mode was reported.

5.1. Inhibitory Effect of Flywheel

Although the loading torque was functioned on BR directly, vibration of No.2 belt was related to both TR and DR. The four rollers were attached to a flywheel with inertia 39 times of DR separately. The ratios of evaluation function and standard one J_6/J_{6_std}, J_7/J_{7_std} were used to estimate the suppression effort. The original evaluation functions of the system were $J_{6_std} = 1.013 \times 10^{-10}$, and $J_{7_std} = 1.947 \times 10^{-7}$.

Table 3 and table 4 expressed the results combining flywheel inertia and adding location. The first row indicated different rollers, and the first column listed different flywheel inertia ratio μ_F, and numbers in red indicated the suppression results achieved 30 % decrement.

It was shown that adding flywheel on burden roller could reduce both the stretching displacement and absolute displacement significantly, especially the former one. Meanwhile the inertia of flywheel affected the inhibition results which was flywheel with larger inertia could achieve better performance. However the disadvantage in this device was that the large inertia would be another burden to the whole system.

5.2. Inhibitory Effect of Dynamic Vibration Absorber

Based on the original system performance, the first and second mode contributed mostly in system vibration. Compensation to these two modes made by dynamic vibration absorber separately were applied to the system on DR. Also in order to reduce additional inertia to the system, μ_a was set to 0.2. Figure 9 and 10 pictured results under different mode compensation with optimal coefficients of stiffness and damping about the absorber. And the evaluation function ratios were listed in table 5.

The coefficients were different when adjusting different modes. For the first mode $k_e = 1.06$, $c_e = 2.5$, and for the second mode $k_e = 0.49$, $c_e = 4.4$.The results indicated that dynamic vibration absorber could suppress both two displacement with a low inertia. Also the absolute displacement which was more concerned with image misalignment was reduced 32% by compensating on the first mode. The disadvantage of dynamic vibration absorber was that it could only inhibit the specific mode due to its working principle. Further more, the coefficients also affected the results. Figure 11 pictured the evaluation function results of stretching displacement with different k_e, c_e that the first mode was attenuated.

It was shown that the optimization of the parameters was also important when designing dynamic vibration absorber. The proper value from mathematical certification remained in the future study.

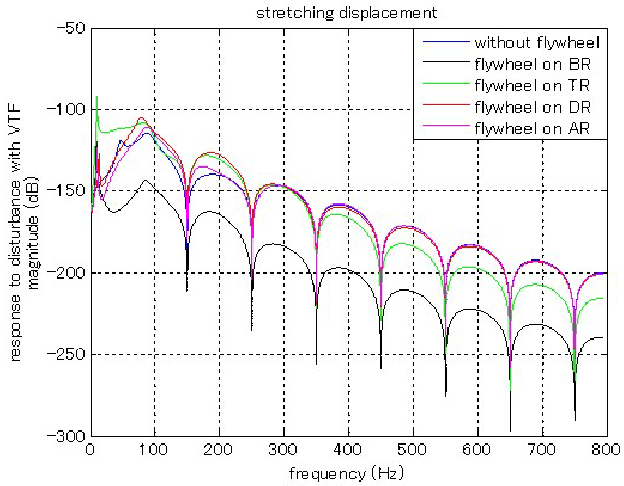

Fig. 7 Stretching displacement with flywheel on different rollers

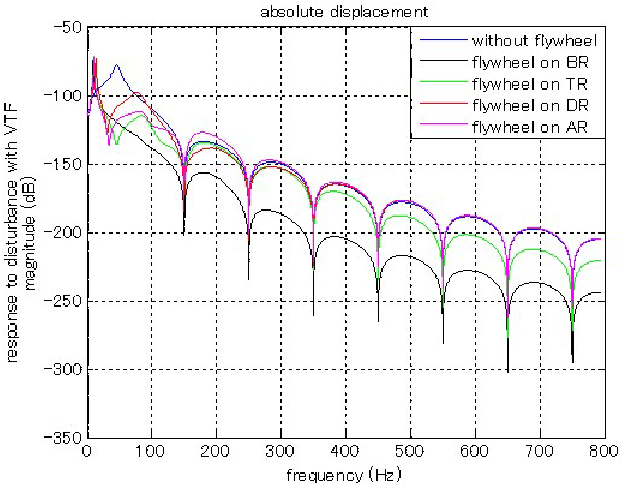

Fig. 8 Absolute displacement with flywheel on different rollers

Roller	Without	on BR	on TR	on DR	on AR
(J_6/J_{6_std})	1	0.0066	10.35	6.261	1.947
(J_7/J_{7_std})	1	0.190	0.201	0.270	0.183

Table 2 Evaluation function ratios by adding flywheel.

6. Conclusion

The present research was carried out on a four-rollers-belt system which was a simplified model of the current widely used intermediate transfer belt (ITB) in colour printing technology. During colour printing procedure, the misalignment occurred on ITB is closely related to the final image quality. Former researches paid more attention on the control strategy of the whole printer system, and little has mentioned about the specific disturbance caused by loading torque of printing medium.

In this study, suppression methods were investigated to attenuate vibration caused by the loading torque. Mathematical descriptions of the four-rollers-belt system and excitation force were established. Meanwhile several comparisons were conducted to investigate the effect of parameters on system behavior. Considering low cost and flexible structure, flywheel and dynamic vibration absorber were applied to the system to suppress the vibration from No. 2 belt mainly which reflected in stretching displacement and absolute displacement. Also in order to estimate the inhibitory effect, an evaluation function containing both system information and human visual sensibility was defined. Cases with varied attaching roller, different inertia, and compensation mode were studied.

	on BR	on TR	on DR	on AR
$\mu_f = 0.05$	0.935	1.132	1.076	1.026
$\mu_f = 0.1$	0.876	1.282	1.153	1.051
$\mu_f = 0.2$	0.774	1.624	1.305	1.097
$\mu_f = 0.3$	0.688	2.010	1.456	1.139
$\mu_f = 0.4$	0.615	2.423	1.604	1.176
$\mu_f = 0.5$	0.553	2.851	1.748	1.210
$\mu_f = 1$	0.350	4.973	2.404	1.340
$\mu_f = 19$	0.014	12.580	5.982	1.897
$\mu_f = 39$	0.0066	10.350	10.350	1.947
$\mu_f = 59$	0.0043	9.312	6.355	1.965
$\mu_f = 79$	0.0033	8.698	6.402	1.974

Table 3 Evaluation function ratio of stretching displacement

	on BR	on TR	on DR	on AR
$\mu_f = 0.05$	1.005	1.003	0.999	1.000
$\mu_f = 0.1$	1.010	1.003	0.998	0.998
$\mu_f = 0.2$	1.014	1.003	0.994	0.994
$\mu_f = 0.3$	1.015	1.000	0.990	0.988
$\mu_f = 0.4$	1.001	0.995	0.985	0.979
$\mu_f = 0.5$	1.005	0.988	0.980	0.969
$\mu_f = 1$	0.956	0.938	0.942	0.908
$\mu_f = 4$	0.701	0.690	0.714	0.644
$\mu_f = 19$	0.353	0.368	0.390	0.335
$\mu_f = 39$	0.190	0.201	0.270	0.183
$\mu_f = 59$	0.127	0.137	0.196	0.125
$\mu_f = 79$	0.100	0.102	0.157	0.093

Table 4 Evaluation function ratio of absolute displacement

Results indicated that rotational stiffness between drive roller and stepper motor affected both stretching displacement and absolute displacement. When adding flywheel with large inertia ($\mu_f = 39$) on burden roller, significant reduction on both displacements could be achieved. Meanwhile dynamic vibration absorber with low inertia ($\mu_a = 0.2$) on drive roller could suppress vibration down to 70% from the originality. Also the coefficients in dynamic vibration absorber parameters affected the suppression results.

The advantages of the methods proposed in this study was the simple structure and low production cost. However flywheel would cause large additional inertia to the system. Meanwhile the system didnt consider the vibration from the stepper motor. Also controlling design on stepper motor will improve the results since the rotational stiffness is one of the vulnerable factors to the system. Further studies will focus on modeling consummation and controller design in dynamic.

Acknowlegement

The corresponding author would like to greatly appreciate for the support of this work from Fuji Xerox Co., Ltd and Tokyo Institute of Technology.

References

(1) C.-L. Chen, and G. T.-C. Chiu, “Banding artifact reduction for a class of color electrophotographic printers with underactuated motor/gear configuration”, IEEE Transactions on Control System Technology, vol. 16, no. 4, pp.577-588, July 2008.

(2) K. Tagawa, Y. Matsuzaki, and T. Kato, “Image formation system including an intermediate transfer belt and method for sensing and correcting speed and position variations of the belt”, Technical Report from Fuji Xerox Co., Ltd., Tokyo, Japan, 1997.

(3) H. Kawamoto, “Transient vibration of a laser scanner motor in digital electrophotography”, Proc. Image Process., Image Quality, Image Capture, Syst. Conf. (PICS), Portland, OR, Mar. 2000, pp. 17-21

(4) H. Kawamoto, K. Udagawa, and M. Mori, “Vibration and noise induced by electrostatic

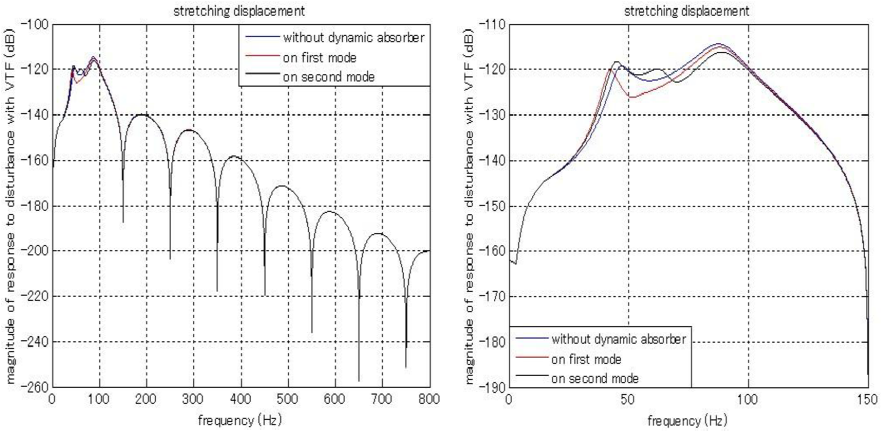

Fig. 9 Stretching displacement with dynamic vibration absorber

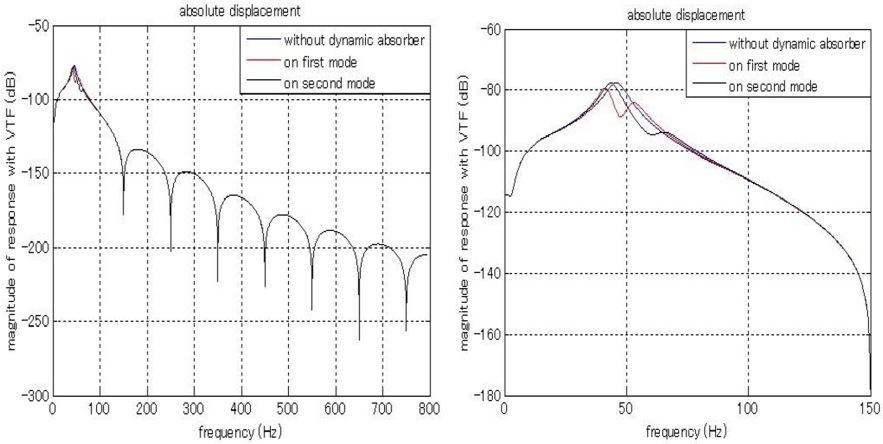

Fig. 10 Absolute displacement with dynamic vibration absorber

Compensation mode	first mode	second mode
(J_6/J_{6_std})	0.8125	0.8126
(J_7/J_{7_std})	0.6802	0.8638

Table 5 Evaluation function ratios by adding flywheel.

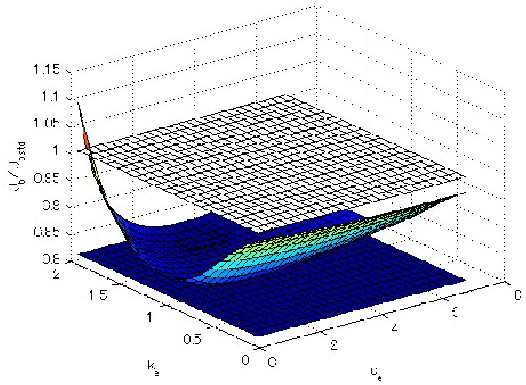

Fig. 11 Results with different

force on a contact charger roller of electrophotography", J. Image Sci. Technol., vol. 39, no. 6, pp. 477-480, Dec. 1995.

(5) D.A. DeHollander, M.S. Roetker, S.J. Griffin, D.W. Martin, and J. Herko, "Intermediate transfer belt and methods for making the same", United States Patent, no. US 7,957,684 B2, Jun.7, 2011

(6) M.T.S. Ewe, G.T.-C, Chiu, J. Grice, J.P. Allebach, C.S. Chan, and W. Foote, "Banding

reduction in electrophotographic process using piezoelectric actuated laser beam deflection device", J. Imagin Sci. Technol., vol. 46, no. 5, pp. 433-442, Sept/Oct. 2002.

(7) G.-Y. Lin, J.M. Grice, J.P. Allebach, G.T-C. Chiu, W. Bradburn, and J. Weaver, "Banding artifact reduction in electrophotographic printers by using pulse width modulation", J. Imaging Sci. Technol., vol. 46, no. 4, pp. 326-337, Jul/Aug. 2002.